2007

Structural and electrical properties of Pb(Zr,Ti)O3 films grown by molecular beam epitaxy

N. Izyumskaya
Virginia Commonwealth University, nizioumskaia@vcu.edu

Vitaliy Avrutin
Virginia Commonwealth University, vavrutin@vcu.edu

X. Gu
Virginia Commonwealth University

See next page for additional authors

Izyumskaya, N., Avrutin, V., Gu, X., et al. Structural and electrical properties of Pb(Zr,Ti)O3 films grown by molecular beam epitaxy. Applied Physics Letters, 91, 182906 (2007).

Structural and electrical properties of $Pb(Zr,Ti)O_3$ films grown by molecular beam epitaxy

N. Izyumskaya,[a] V. Avrutin, X. Gu, B. Xiao, S. Chevtchenko, J.-G. Yoon,[b] and H. Morkoç
Department of Electrical and Computer Engineering, Virginia Commonwealth University, Richmond, Virginia 23284, USA

Lin Zhou and David J. Smith
Deptartment of Physics, Arizona State University, Tempe, Arizona 85287, USA

(Received 23 August 2007; accepted 11 October 2007; published online 31 October 2007)

Single-crystal, single-phase $Pb(Zr_xTi_{1-x})O_3$ films (x=0–0.4) were grown on (001) $SrTiO_3$ and SrTiO3:Nb substrates by molecular beam epitaxy. Layer-by-layer growth of the $Pb(Zr,Ti)O_3$ films was achieved by using $PbTiO_3$ buffer layers between the $SrTiO_3$ substrates and the $Pb(Zr,Ti)O_3$ films. The layers with low Zr content showed high crystallinity with full width at half maximum of ω-rocking curves as low as 4 arc min, whereas increase in Zr concentration led to pronounced angular broadening. The $PbZr_{0.07}Ti_{0.93}O_3$ films exhibited remanent polarization as high as 83 $\mu C/cm^2$, but local areas suffered from nonuniform leakage current. © *2007 American Institute of Physics*. [DOI: 10.1063/1.2804571]

Due to their attractive properties[1] such as large piezoelectric coefficient, electrical polarization, and electromechanical coupling factor, ferroelectric $Pb(Zr_xTi_{1-x})O_3$ (PZT) thin films are of considerable current interest for a wide range of applications, among which are the gate material for field effect transistor based ultrasonic and motion sensors, infrared detectors, surface acoustic wave devices, microactuators, ferroelectric field effect transistors, and nonvolatile ferroelectric random access memory devices, as well as a plethora of applications in nonlinear optics. To exploit the unique properties of PZT for device applications, high-quality single-crystal films are required. Epitaxial PZT thin films have been prepared by various methods such as sol-gel[2,3] and hydrothermal[4,5] techniques, metal-organic chemical vapor deposition,[6,7] rf magnetron sputtering,[8,9] and pulsed laser deposition.[10] However, the growth of single-crystal PZT films by molecular beam epitaxy (MBE), a modern technique providing high crystal perfection and precise control over material composition, has not been yet reported. In this letter, we report on the growth of high-quality single-crystal PZT layers by peroxide MBE (the method developed previously for ZnO growth[11]) and their structural and ferroelectric characteristics.

The PZT layers were grown on (001) $SrTiO_3$ substrates in a modified Riber 3200 MBE system. A 50% aqueous solution of hydrogen peroxide (H_2O_2) was employed as a source of reactive oxygen, while 99.999% pure Pb and 99.995% pure Ti were supplied from double-zone and high-temperature effusion cells, respectively. Due to the very low equilibrium pressure of metallic Zr, a metal-organic source of Zr was used. Zirconium tetra butoxide was chosen as the precursor, and 6N-purity Ar was used as the carrier gas. Before loading into the chamber, the $SrTiO_3$ substrates were etched in a buffered NH_4F–HF solution, rinsed in de-ionized water, and dried with nitrogen. The substrates were loaded into the air lock, followed by the growth chamber, and then heated to and kept at 600 °C for 20 min under a H_2O_2/H_2O vapor pressure of 1×10^{-5} Torr. PZT layers were grown at a H_2O_2/H_2O pressure of about 5×10^{-5} Torr, a substrate temperature of 600–625 °C, and a Pb-to-Ti flux ratio of >1. The thicknesses of the layers measured with an Alpha-step 250 profilometer were in the range of 40–80 nm. The PZT film composition was determined by Rutherford backscattering spectroscopy (RBS).

The growth process was monitored *in situ* by reflection high-energy electron diffraction (RHEED). Spotty RHEED patterns were observed for PZT films at the beginning of the growth on $SrTiO_3$ due to a three-dimensional (3D) growth mode, leading to rough surface morphology. The spotty RHEED patterns of the PZT films became progressively worse with further deposition, with the spots transforming into short arcs as an indicative of textured polycrystalline films. To overcome this problem, a $PbTiO_3$ buffer layer was introduced between the $SrTiO_3$ substrate and the PZT film. As a result, PZT layers grown on $PbTiO_3/SrTiO_3$ templates showed streaky RHEED patterns, characteristic of two-dimensional (2D) growth and smooth film surfaces. The $PbTiO_3$ buffer worked well for PZT layers with low Zr concentration (up to ~10%), but PZT films with higher Zr content (up to ~40% Zr) showed more complex behavior. Initially, 2D RHEED patterns were observed, which switched to 3D patterns as growth progressed, then returning to 2D patterns, as illustrated in Fig. 1. The higher the Zr content was, the earlier the 2D-3D transition started and the more pronounced the 3D pattern was. The MBE growth and characterization of the ternary compounds $PbTiO_3$ and $PbZrO_3$ are described in more detail elsewhere.[12,13]

Phase composition and structural properties of the films were determined by x-ray diffraction (XRD) and RBS. XRD studies revealed that the PZT films were single-phase and c-axis oriented. Figure 2 presents a ω-2θ scan of a $PZT/PbTiO_3/SrTiO_3$ structure. Only the (00l) reflections of the substrate and the layers are visible. However, (h00) reflections of tetragonal PZT with low Zr content should vir-

[a]Electronic mail: nizioumskaia@vcu.edu
[b]Present address: Department of Physics, University of Suwon, Kyounggi-do 445-743, Korea.

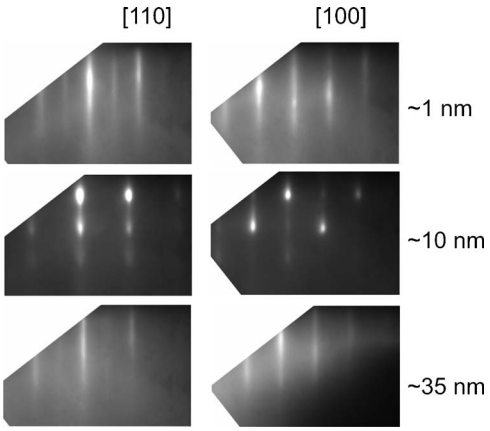

FIG. 1. RHEED pattern evolution during MBE growth of $Pb(Zr_{0.3}T_{0.7})O_3$ film on $SrTiO_3$ substrate with $PbTiO_3$ buffer layer.

tually coincide with (00*l*) reflections from the $SrTiO_3$ substrate. Therefore, to detect *a*-axis-oriented regions (*a* domains) possibly present in the films, rocking curves (ω scan) were measured at the 2θ angle corresponding to $PbTiO_3(100)$ reflection overlapping with the $SrTiO_3(001)$ reflection.[14,15] Only the diffraction peak corresponding to the substrate was observed, and no evidence of *a* domains was found. XRD and RHEED data indicated that the PZT layers exhibited the epitaxial relationship $PZT(100)\|SrTiO_3(100)$ and $PZT[001]\|SrTiO_3[001]$. The measured full width at half maximum of (001) ω-rocking curve for an 80-nm-thick $PbZr_{0.07}Ti_{0.93}O_3$ film was as low as 4 arc min, as compared to 2.3 arc min for the substrate, indicative of the high crystal quality of the epitaxial layer. However, increase in Zr content resulted in broadening of the XRD rocking curves up to 24 arc min for a $PbZr_{0.4}Ti_{0.6}O_3$ film. The out-of-plane and in-plane lattice parameters calculated from the 2θ positions of symmetrical (001) and asymmetrical (101) XRD reflections were $a=3.93$ Å and $c=4.19$ Å for $PbZr_{0.4}Ti_{0.6}O_3$ and $a=3.88$ Å and $c=4.17$ Å for PZT layers containing 7% Zr. The c/a ratio decreases slightly from 1.075 to 1.066 as the Zr content increases from 7% to 40%. The values of the c/a ratio for our films are higher than those for PZT bulk ceramics of the same compositions (1.057 and 1.035 for 7% and 40% Zr, respectively[16]), which is indicative of biaxial compressive strain in the films. It is interesting to note that the *a* parameter for the $PbZr_{0.07}Ti_{0.93}O_3$ layers is very close to the bulk *a* parameter for $PbTiO_3$, suggesting that the $PbZr_{0.07}Ti_{0.93}O_3$ films are pseudomorphic to the $PbTiO_3$ buffer layers.

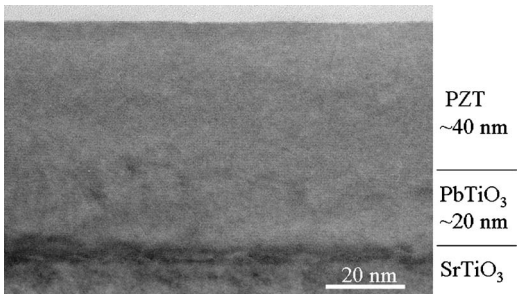

FIG. 3. Cross-sectional electron micrograph of $Pb(Zr_{0.07}T_{0.93})O_3$ film grown on $PbTiO_3$ buffer layer on $SrTiO_3$ substrate.

The film microstructure was further examined by transmission electron microscopy (TEM). Figure 3 shows a cross-sectional electron micrograph of a $PbZr_{0.07}Ti_{0.93}O_3/PbTiO_3/SrTiO_3$ structure. Misfit dislocations are visible at the $PbTiO_3/SrTiO_3$ interface, but there is no distinct boundary between the $PbTiO_3$ buffer and the PZT layer, confirming that the $PbZr_{0.07}Ti_{0.93}O_3/PbTiO_3$ bilayer structure had partially relaxed as a whole by introduction of the misfit dislocations at the $PbTiO_3/SrTiO_3$ interface. It should also be mentioned that no *a* domains were visible in the electron micrographs, in agreement with the XRD data.

The PZT films were also grown on conductive, Nb-doped $SrTiO_3$ substrates in order to examine their ferroelectric properties. Au/Pt top electrodes of 30 nm/30 nm in thickness and 300 μm in diameter were deposited by e-beam evaporation. Polarization versus applied electric field (*P-E*) characteristics were measured at room temperature with a Radiant Technologies Precision LC ferroelectric test system. Figure 4 shows the *P-E* hysteresis loop for a 70-nm-thick $PbZr_{0.07}Ti_{0.93}O_3$ film grown on a thin (6 nm) $PbTiO_3$ buffer layer. The remanent polarization is 83 $\mu C/cm^2$, and the coercive field is 77 kV/cm. It should be mentioned, however, that current-voltage characteristics of the PZT films suffered from high leakage current (from 10^{-4} to 10^{-2} A/cm^2 for an applied bias of 2 V), which resulted in distortion of the hysteresis loop at high fields. High leakage currents have been reported previously for PZT layers with low Zr content (be-

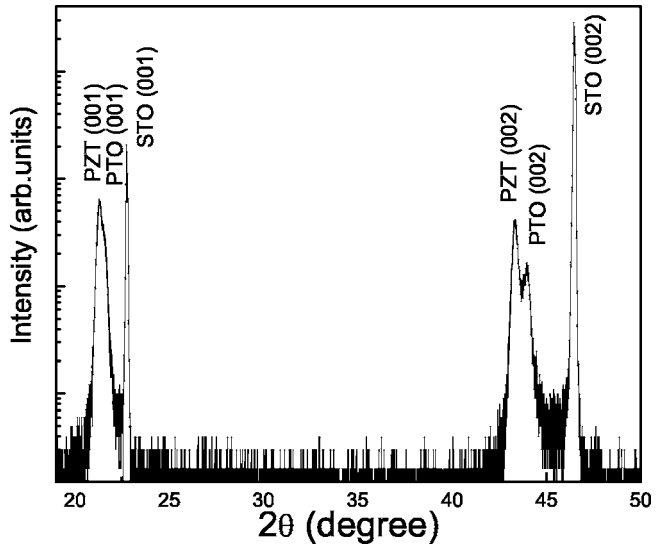

FIG. 2. XRD ω-2θ scan for 60-nm-thick $Pb(Zr_{0.07}T_{0.93})O_3$ film grown on $PbTiO_3$ buffer layer on $SrTiO_3$ substrate.

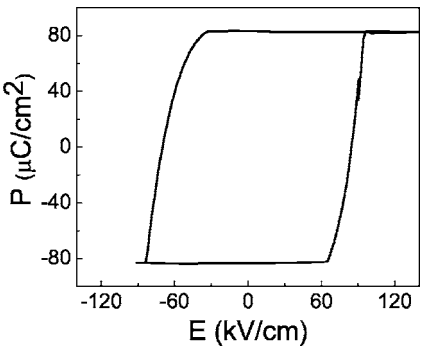

FIG. 4. *P-E* hysteresis curve measured for 70-nm-thick $Pb(Zr_{0.07}T_{0.93})O_3$ film.

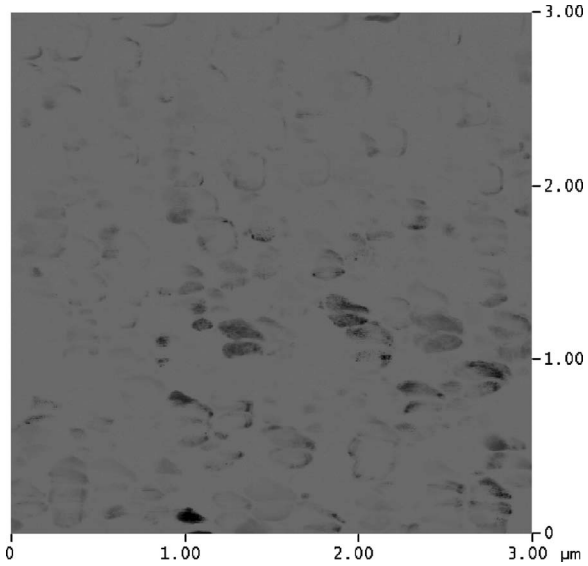

FIG. 5. 3×3 μm^2 C-AFM image for $Pb(Zr_{0.07}T_{0.93})O_3$ film recorded at a bias voltage of −2 V; Δz=4 pA and a mean of −1 pA.

low 30%) by Foster *et al.*,[17] although the source of the high leakage was unclear.

To shed some light on the origin of the electrical leakage in our layers, conductive atomic force microscopy (C-AFM) studies were performed. Figure 5 shows typical C-AFM scan for $PbZr_{0.07}Ti_{0.93}O_3$. The darker tone of the image corresponds to higher current. A nonuniform distribution of electrical current over the sample surface is apparent. Most of the sample surface exhibits current values below the detection limit of our apparatus (~1 pA), but some local areas are highly leaky. Such a distribution of current allows us to assume that structural defects might be responsible for high leakage in the PZT film. These defects could originate from the $SrTiO_3$:Nb substrates, which are known to have inferior crystal quality compared to undoped $SrTiO_3$ substrates. However, second-phase inclusions, such as lead oxide, cannot be ruled out. Further TEM investigation of PZT films grown on conductive substrates is necessary to clarify this issue.

In conclusion, single-crystal, single-phase PZT films were grown on (001) $SrTiO_3$ substrates by peroxide MBE. The use of $PbTiO_3$ buffer layer resulted in layer-by-layer growth of epitaxial PZT films. A nearly square-shaped *P-E* hysteresis loop was observed for a 70-nm-thick $PbZr_{0.07}Ti_{0.93}O_3$ film with a remanent polarization of 83 $\mu C/cm^2$. Nonuniform distribution of leakage current across the films was found by conductive AFM. Defects penetrating from the $SrTiO_3$:Nb substrate and/or second-phase inclusions are presumably responsible for the electrical leakage.

This work was supported by a grant from the Office of Naval Research under the direction of Dr. C. E. C. Wood. We acknowledge use of facilities in the John M. Cowley Center for High Resolution Electron Microscopy at Arizona State University.

[1]P. Muralt, J. Micromech. Microeng. **10**, 136 (2000).
[2]W. Gong, J.-F. Li, X. Chu, Z. Gui, and L. Li, Appl. Phys. Lett. **85**, 3818 (2004).
[3]R. Waser, T. Schneller, S. Horrmann-Eifert, and P. Ehrhart, Integr. Ferroelectr. **36**, 3 (2001).
[4]T. Morita, Y. Wagatsuma, Y. Cho, H. Morioka, and H. Funakubo, and N. Setter, Appl. Phys. Lett. **84**, 5094 (2004).
[5]W. L. Suchanek, M. Lencka, L. McCandlish, R. L. Pfeffer, M. Oledzka, K. Mikulka-Bolen, G. A. Rossetti, Jr., and R. E. Riman, Cryst. Growth Des. **5**, 1715 (2005).
[6]R. Ramesh, S. Aggarwal, and O. Auciello, Mater. Sci. Eng., R. **32**, 191 (2001).
[7]S. Yokoyama, Y. Honda, H. Morioka, S. Okamoto, H. Funakubo, T. Iijima, H. Matsuda, K. Saito, T. Yamamoto, H. Okino, O. Sakata, and S. Kimura, J. Appl. Phys. **98**, 094106 (2005).
[8]S.-M. Nam and T. Tsurumi, Jpn. J. Appl. Phys., Part 1 **43**, 2672 (2004).
[9]D. M. Kim, C. B. Eom, V. Nagarajan, J. Ouyang, R. Ramesh, V. Vaithyanathan, and D. G. Schlom, Appl. Phys. Lett. **88**, 142904 (2006).
[10]T. J. Zhu, L. Lu, and M. O. Lai, Appl. Phys. A: Mater. Sci. Process. **81**, 701 (2005).
[11]N. Izyumskaya, V. Avrutin, W. Schoch, A. El-Shaer, F. Reuss, Th. Gruber, and A. Waag, J. Cryst. Growth **269**, 356 (2004).
[12]X. Gu, N. Izyumskaya, V. Avrutin, H. Morkoç, T. D. Kang, and H. Lee, Appl. Phys. Lett. **89**, 122912 (2006).
[13]N. Izyumskaya, V. Avrutin, X. Gu, Ü. Özgür, B. Xiao, T. D. Kang, H. Lee, and H. Morkoç, *Ferroelectrics and Multiferroics*, MRS Symposia Proceedings No. 966 (Materials Research Society, Pittsburgh, 2007), p. 0966-T11-17.
[14]Z. Li, M. Foster, D. Guo, H. Zhang, G. R. Bai, P. M. Baldo, and L. E. Rehn, Appl. Phys. Lett. **65**, 1106 (1994).
[15]M. de Keijser, D. M. de Leeuw, P. J. van Veldhoven, A. E. M. De Veirman, D. G. Neerinck, and G. J. M. Dormans, Thin Solid Films **266**, 157 (1995).
[16]G. Shirane and K. Suzuki, J. Phys. Soc. Jpn. **7**, 333 (1952).
[17]C. M. Foster, G.-R. Bai, R. Csencsits, J. Vetrone, R. Jammy, L. A. Wills, E. Carr, and J. Amano, J. Appl. Phys. **81**, 2349 (1997).